DOI 10.31489/2020No2/11-18

UDC 538.956

VARIATION OF STRUCTURAL PROPERTIES OF Al DOPED Ni-Cd FERRITES WITH SINTERING TIME

Halamani Koushallya M.[1], Mathad Shalini K.[1], Kulkarni Akshay B.[2], Mathad Shridhar N.[3], Jeergal Pundalik. R.[1], Hiremath Chidanandayya.S.[4], Pujar Appanna S.[5], Pujar Rangappa B.[1*]

[1]P.C. Jabin Science College, Karnataka, India

[2]South Konkan Education Society's (SKES's) Govindram Seksaria Science College, Belagavi, India

[3]Karnataka Lingayat Education (K.L.E) Institute of Technology, Gokul, Hubballi, Karnataka, India, physicssiddu@gmail.com,

[4]Shri Kadasiddheshwar Arts College & H.S.Kotambri Science Institute, Vidyanagar, Hubballi, India

[5] Raja Lakhamagouda Science Institute, Belgavi, India, p_rangappa@rediffmail.com

The aim of present work is to synthesis and study the structural properties of Al doped Ni-Cd ferrites, series by ceramic method. The samples are sintered at a temperature of 1100 C with sintering time of t=9, 11, 13, 15 hrs. The samples were characterized by X-ray diffraction, scanning electron microscope, energy dispersive X-ray analysis and Fourier transform-Infrared. The single phase simple cubic spinel structure is confirmed by X-ray diffraction patterns. The lattice parameter is found to be in the range of 8.478 Å - 8.481 Å. The uniform size distribution is observed in the scanning electron microscope micrographs. The elemental analysis is done by energy dispersive X-ray analysis confirming the presence of all the metal ions present in the ferrite formula. Fourier transform-Infrared spectra showed two bands υ_1 (581-582 cm^{-1}) and υ_2 (less than 400 cm^{-1}) which are attributed to metal oxygen bond vibrations at tetrahedral and octahedral sites respectively.

Keywords: X-ray diffraction, scanning electron microscope, energy dispersive X-ray analysis, Fourier transform-Infrared

Introduction

Ferrites are an attractive class of research materials because of their comprehensive physical properties and application in advanced technology. Modification of their structure has been shown to play an important role in the optimization of their structural, optical and electrical properties [1-2]. Cubic spinel ferrites are chemical compounds with the formula of AB_2O_4, where A and B represent various metal cat-ions, usually including iron. In the normal spinel structure, the 8 divalent metal ions go into the A sites, and the 16 trivalent iron ions have preference for B sites [1]. Among the magnetic materials that have found broad practical application in technology, ferrites deserve attention [2].

Cobalt ferrite ($CoFe_2O_4$) has attracted much attention owing to its excellent properties, such as its relatively high saturation magnetization (M_s), high coercivity (H_c), magnetic anisotropy, good chemical stability and good catalytic activity. Its physical properties are strongly dependent on the cation distribution among the tetrahedral (A) and the octahedral (B) sites in the crystal lattice. Depending upon the distribution of the various cat-ion substituents over tetrahedral and octahedral sites, its magnetic and electrical properties can be modified according to the research interest [3].

Spinel ferrite is known to be good candidate for magnetic recording and microwave applications [4]. Nano-sized grains of ferrite are being applied in permanent magnets [5], magnetic drug delivery [6], and high-density information storage [7]. Soft magnetic material have a widespread applications in recording heads, antenna rods, loading coils, microwave devices, core material for power transformers due to their high resistivity and low eddy current losses [8]. Ferrite materials can be prepared by numbers of methods such different routes like co-precipitation [9],solid state reaction [10-11], citrate precursor [12], sol–gel and auto-combustion [13], ball milling [14] hydrothermal [15].

This paper presents the influence of sintering time with the general chemical formula $Ni_{0.5}Cd_{0.5}Al_{0.1}Fe_{1.9}O_4$ series which are prepared by ceramic method. Using X-ray diffraction (XRD), scanning

electron microscope (SEM), energy dispersive X-ray analysis (EDAX) and Fourier transform-Infrared (FT-IR) analysis, detailed structural and mechanical properties of crystalline Ni-Cd-Al spinel ferrites reported in this paper.

1. Experiments

In photo acoustic effect, interaction of electromagnetic radiation with matter generates sound. This effect consists of the absorption of incident radiation by target molecule. Photo acoustic effect is popular due to a minimal sample preparation during execution, the ability to examine scattering and opaque sample [12] along with the capability to access depth profile [13]. The ferrites with general chemical formula $Ni_{0.5}Cd_{0.5}Al_{0.1}Fe_{1.9}O_4$ were synthesized by ceramic method using AR grade Nickel oxide, Cadmium oxide, and Ferric oxide in molar preparation and mixed mechanically in agate motor in acetone medium as shown in Fig.1. Then the ferrites were pre sintered with temperature constant 1100ºc for different time 9 hours, 11 hours, 13 hours, and 15 hours.

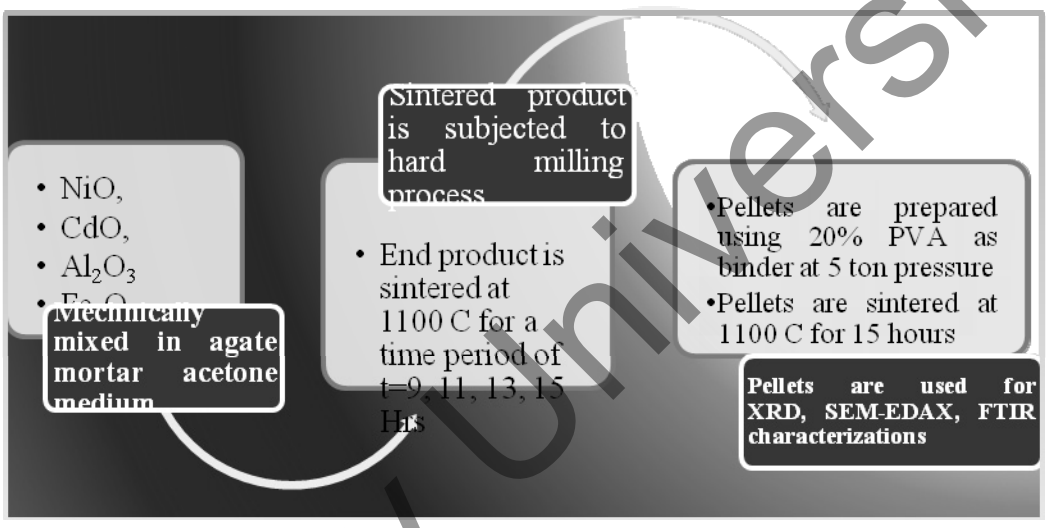

Fig.1. Flow chart of synthesis of ferrite samples using ceramic method.

The pre sintered powders were subjected to hard milling process in acetone medium. One or two drops of PVA solution of 20% concentration was added as binder. All the samples were pressed into two pellets of 1cm in diameter and 0.2 cm in height by applying a pressure of about 5tons/square inch for 5 minutes. The pellets were subjected to final sintering at 1100ºc for 15 hours.

The Structural characterization of the ferrite pellets is carried out the X-ray diffraction patterns of the samples have been obtained on Bruker AXS D8 Advance Diffractometer (XRD), (with Cu-K_α radiation, wavelength, λ= 1.5406 Å), the SEM-EDAX spectrographs of the samples have been obtained on JEOL Model JSM - 6390LV and the FTIR of the samples have been obtained on Thermo Nicolet, Avatar 370.

2. Results and Discussion

2.1. X-ray diffraction (XRD) analysis

XRD patterns of the $Ni_{0.5}Cd_{0.5}Al_{0.1}Fe_{1.9}O_4$ (t=9, 11, 13, 15 hrs) ferrite series is shown in Fig.2. The peaks matched well with those from the Joint Committee on Powder Diffraction Standards (JCPDS) card no.00-022-1086. The reflections observed from the planes (220), (311), (400), (422), (511), (440) and (533) for the samples confirm the formation of a cubic spinel structure.

The lattice parameter of all the samples was calculated and the values are given in Table 1. The lattice parameter was found to remain constant. The hopping length; the bond length, ionic radii and the value of X-ray density (Δx) and stacking fault coefficient were calculated elsewhere [10, 11] and the values are tabulated in Table 1. The actual density is calculated using standard method. The values are tabulated in Table 1.

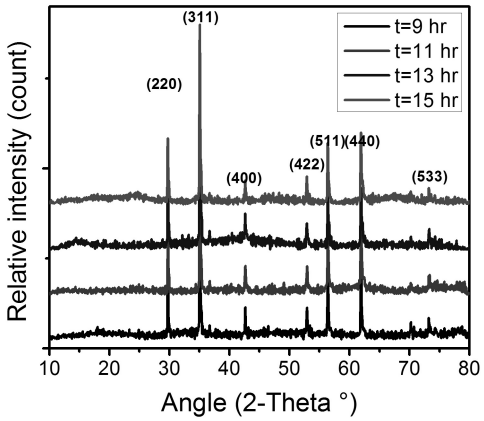

Fig.2. XRD graph of $Ni_{0.5}Cd_{0.5}Al_{0.1}Fe_{1.9}O_4$ferrite synthesized by ceramic method.

Table 1 - Calculated values of lattice parameter, volume of unit cell, hopping length, bond length, ionic radii, stacking fault coefficient, x-ray density, actual density and porosity.

Sintering time (t)	**9 hr**	**11 hr**	**13 hr**	**15 hr**
Lattice parameter a (Å)	8.48	8.47	8.48	8.48
Volume of unit cell V (10^{-30} m^{-3})	609	608	609	610
Hopping length L_A (Å)	3.67	3.67	3.67	3.67
Hopping length L_B (Å)	3.00	3.00	3.00	3.00
Bond Length A-O (Å)	1.94	1.94	1.94	1.94
Bond length B-O (Å)	2.06	2.06	2.06	2.06
Ionic Radii r_A (Å)	0.59	0.59	0.59	0.59
Ionic Radii r_B (Å)	0.71	0.71	0.71	0.71
Stacking fault coefficient α (10^{-3})	0.43	0.45	0.36	0.53
x-ray density Δx (gr/cm^3)	5.63	5.64	5.63	5.63
Actual density d_a (gr/cm^3)	4.38	3.51	3.82	3.76
Porosity (%)	22.24	37.67	32.17	33.25

The crystallite size of ferrite samples was calculated by using Debye-Scherrer [10, 11] equation $D = 0.9 \cdot \lambda / \beta_D \cos\theta$, where D is the crystallite size, β_D is pure diffraction broadening given by the full width half maximum (FWHM) of the peaks, λ is the wavelength of the radiation used, θ is the angle of diffraction. The Dislocation density calculated using two different formulas $\rho_D = 1/D^2$, $\rho_D = 15\varepsilon/aD$ and micro-strain calculated using $\varepsilon = \beta\cos\theta/4$ are also tabulated in Table 2.

Table 2 - Calculated values of crystallite size, micro strain and dislocation density using WH plots, SSP and standard formula.

	Crystallite size (in Å)			Micro strain (10^{-3})			Dislocation density (ρ) (10^{14})	
Sintering time t in hr	From WH graph	From SSP	From formula	Micro strain ε=slope/4 (WH)	Micro strain ε=2*sqrt (intercept) (SSP)	From formula ε=βcosθ/4	$\rho=1/D^2$	$\rho=15\varepsilon/aD$
9	835	651	522	0.61	4.43	0.67	3.84	2.28
11	766	700	439	0.84	7.40	0.81	5.55	3.26
13	462	415	457	0.11	1.81	0.80	5.61	3.09
15	510	501	503	0.05	1.76	0.70	4.22	2.47

2.2. Williamson Hall (WH) plot and Size-Strain (SS) Plot Method

The distinct θ dependencies of size and strain broadening of the diffraction lines laid the basis for Williamson and Hall method (WH). An additional component $\beta_s = 4\varepsilon \tan\theta$ to the Scherrer equation results in WH equation $\beta_{hkl}\cos\theta = \frac{K\cdot\lambda}{D} + 4\varepsilon\sin\theta$, [11, 16].

The WH plots for the $Ni_{0.5}Cd_{0.5}Al_{0.1}Fe_{1.9}O_4$ (t= 9, 11, 13, 15 hrs) are shown Fig. 3 (a-d).

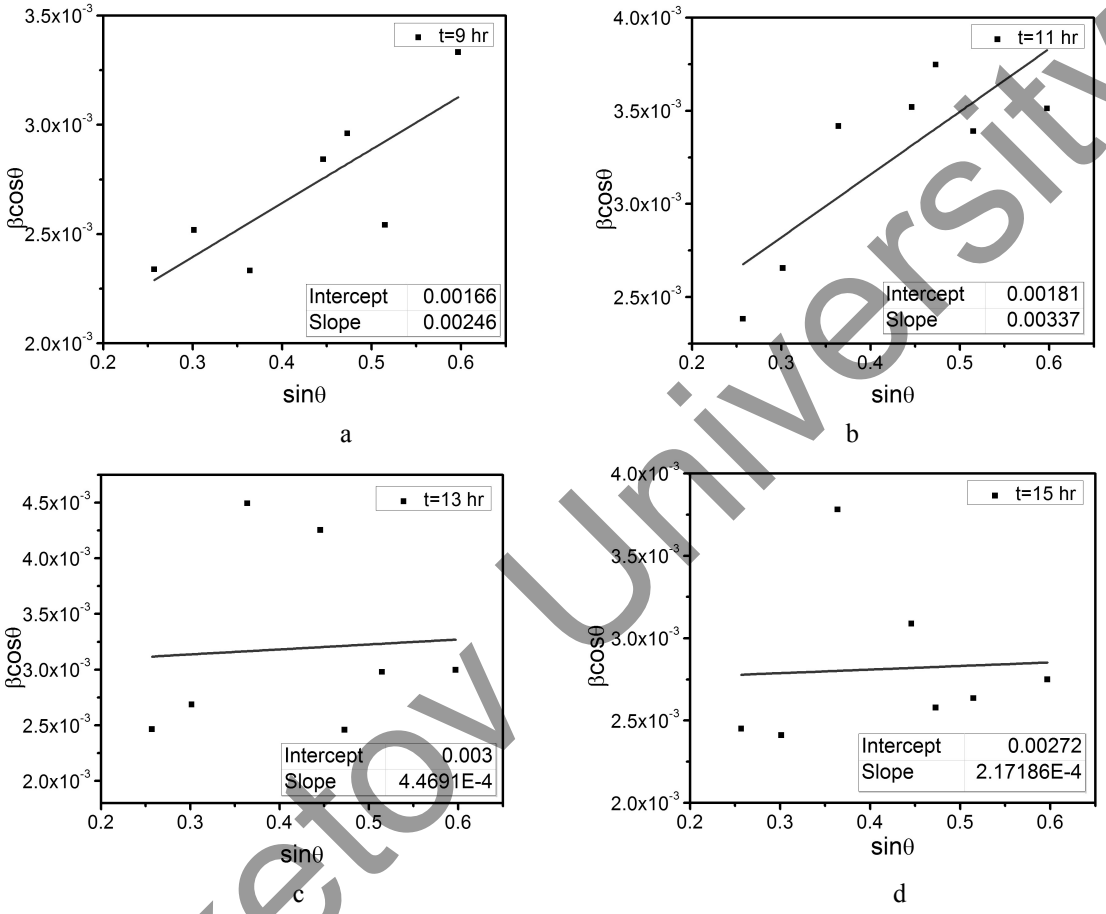

Fig.3. WH plots of $Ni_{0.5}Cd_{0.5}Al_{0.1}Fe_{1.9}O_4$ ferrite series synthesized by ceramic method.

Using the slope and intercept values of the graph of βcosθ with respect to sinθ; the value of crystallite size and microstrain are calculated and are tabulated in the Table 2.

The SS plot is a tool to understand the isotropic nature and micro-strain contribution. The SS plots of $Ni_{0.5}Cd_{0.5}Al_{0.1}Fe_{1.9}O_4$ (t= 9, 11, 13, 15 hrs) ferrite series is shown in Fig. 4 (a-d). In this approximation, crystallite size and strain are having a relation given by the equation $(d_{hkl}\beta_{hkl}\cos\theta)^2 = \frac{K.\lambda}{D}(d_{hkl}^2\beta_{hkl}\cos\theta) + \left(\frac{\varepsilon}{2}\right)^2$, where K is a constant [11, 17-18]. The calculated value of crystallite size and microstrain are tabulated in the Table 2. The microstrain is observed to be decreasing with increase in sintering time. The crystallite size is observed to be steady. All the samples showed the dislocation density in the range of 10^{14}.

2.3. Scanning electron microscope studies

The SEM micrographs of $Ni_{0.5}Cd_{0.5}Al_{0.1}Fe_{1.9}O_4$ (t= 9, 11, 13, 15 hrs) series are shown in the Fig. 5(a-d). The images show uniform distribution of the grains with uniform grain size of the order of 1 μm. The grains are having octahedral and tetrahedral structures showing very sharp boundary growth. The grain size increased with increase in the sintering time.

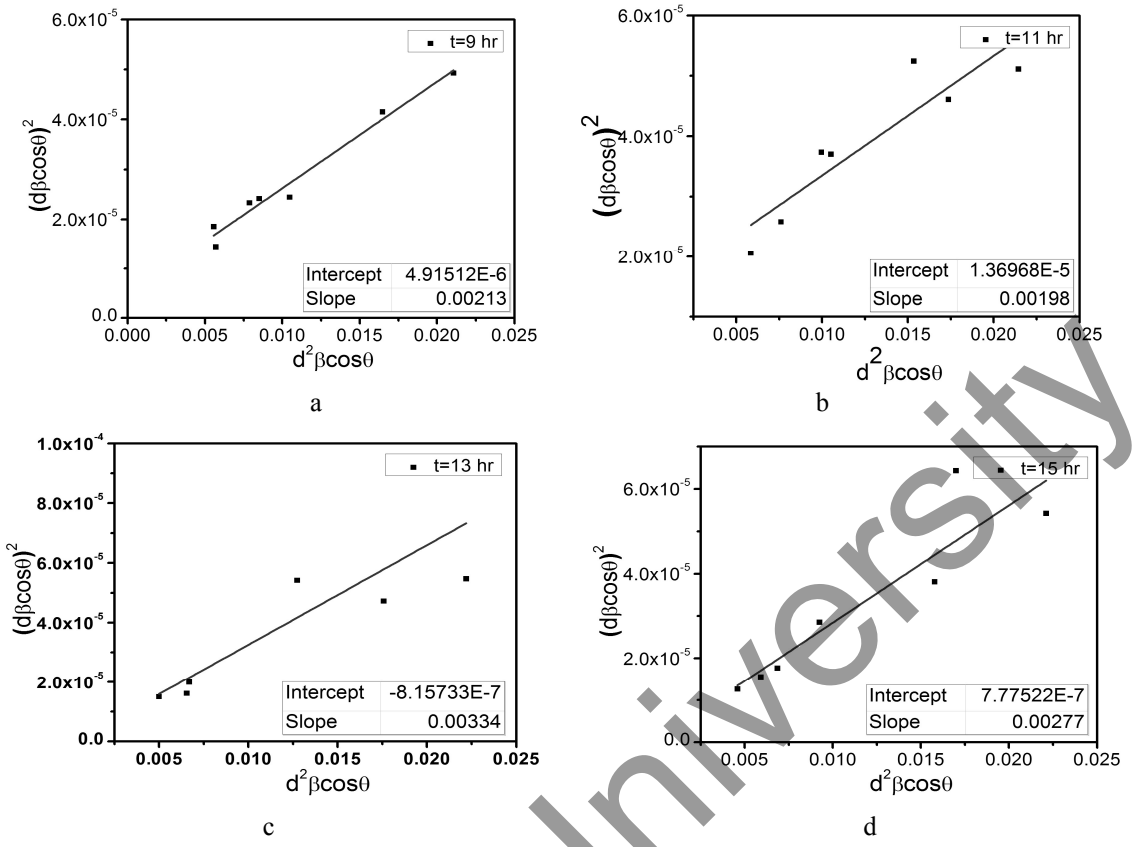

Fig.4. SS plots of $Ni_{0.5}Cd_{0.5}Al_{0.1}Fe_{1.9}O_4$ferrite series synthesized by ceramic method.

The elemental analysis is done by EDAX analysis and the diffraction spectra of $Ni_{0.5}Cd_{0.5}Al_{0.1}Fe_{1.9}O_4$ (t= 9, 11, 13, 15 hrs) series are shown in Fig. 6, a-d.

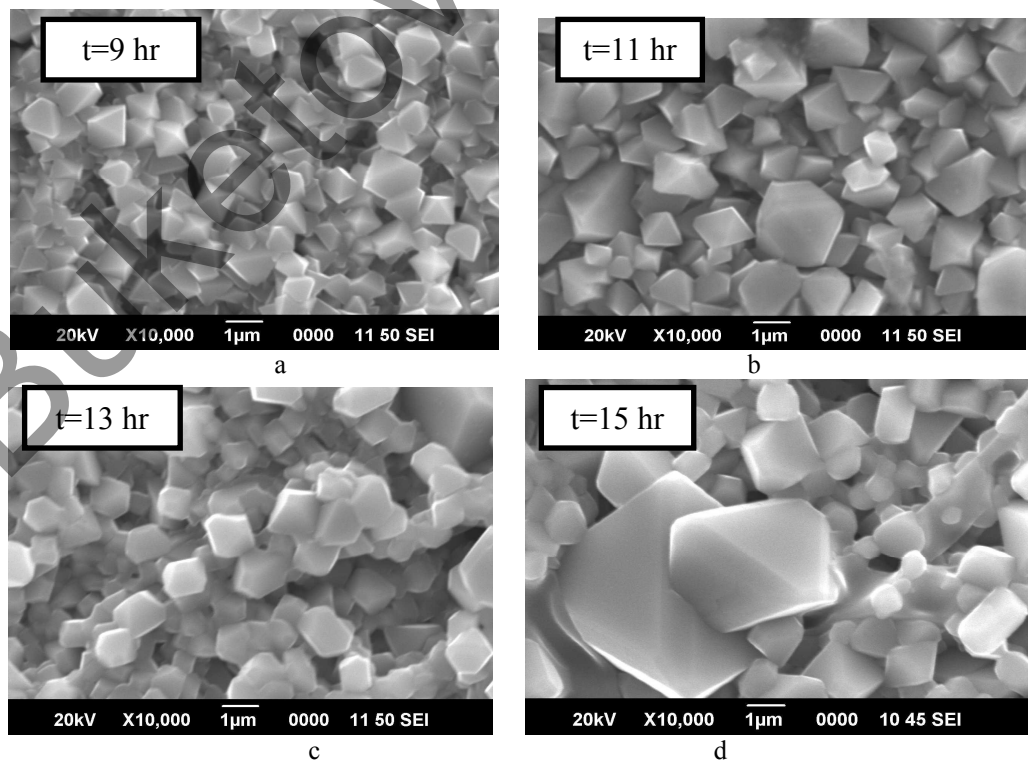

Fig. 5. SEM micrographs of $Ni_{0.5}Cd_{0.5}Al_{0.1}Fe_{1.9}O_4$ ferrite series synthesized by ceramic method.

2.4. Energy dispersive X-ray analysis studies

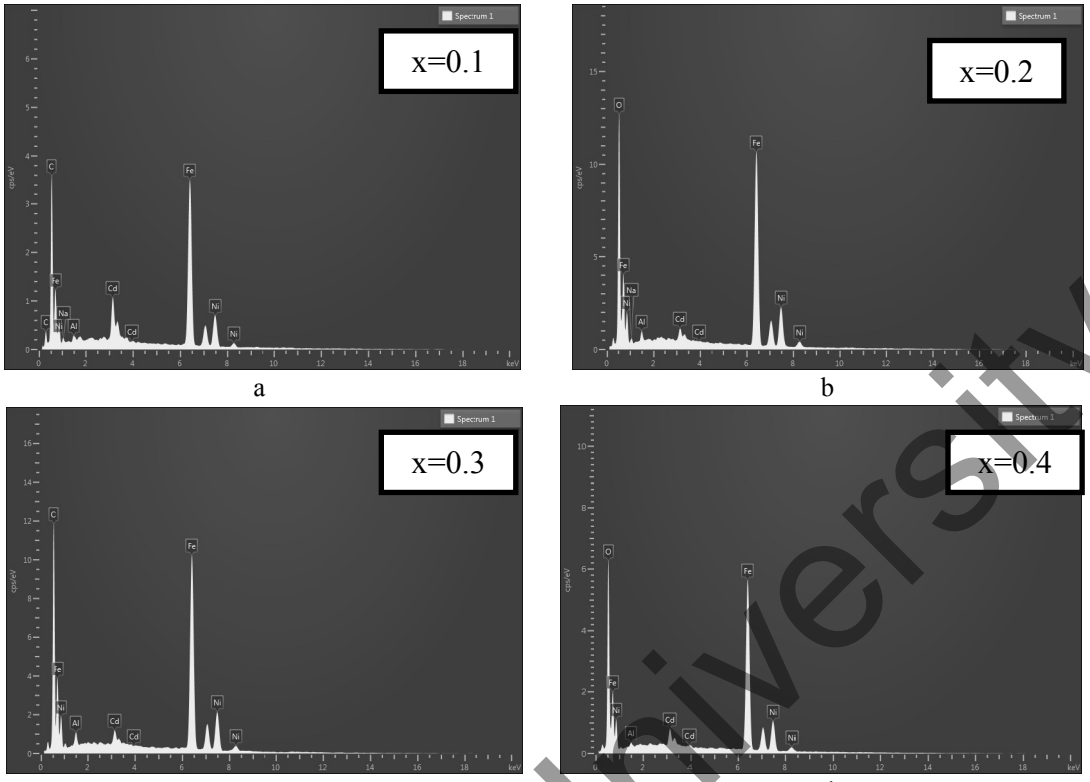

Fig. 6. EDAX of $Ni_{0.5}Cd_{0.5}Al_{0.1}Fe_{1.9}O_4$ ferrite series synthesized by ceramic method.

The spectra confirming the presence of all the metal ions present in the ferrite formula and the atomic proportion tabulated in Table 3.

Table 3 - Initial values of atomic proportions of metal ions taken by stoichio-metric proportion and observed values using EDAX analysis of in the samples of $Ni_{0.5}Cd_{0.5}Al_{0.1}Fe_{1.9}O_4$ ferrite series with sintering time t=9, 11, 13, 15 hrs.

	Weight (%)				Observed atomic proportion using EDAX				Stoichiometric composition taken for synthesis			
	t=9 hr	t=11 hr	t=13 hr	t=15 hr	t=9 hr	t=11 hr	t=13 hr	t=15 hr	t=9 hr	t=11 hr	t=13 hr	t=15 hr
O	25.21	25.33	25.53	25.71	4.056	3.850	3.836	3.890	4	4	4	4
Al	0.52	1.04	1.27	0.46	0.049	0.093	0.113	0.041	0.1	0.1	0.1	0.1
Fe	45.44	52.54	53.53	53.87	2.094	2.288	2.304	2.335	1.9	1.9	1.9	1.9
Ni	13.52	17.17	16.74	15.39	0.593	0.711	0.685	0.635	0.5	0.5	0.5	0.5
Cd	9.07	2.64	2.93	4.57	0.208	0.057	0.062	0.099	0.5	0.5	0.5	0.5
Tot	93.76	98.72	100	100	7.000	7	7	7	7	7	7	7

2.5. Fourier transform infrared (FT-IR) studies

The FT-IR spectra of $Ni_{0.5}Cd_{0.5}Al_{0.1}Fe_{1.9}O_4$ ferrite series with sintering time t=9, 11, 13, 15 hrs Fig. 7. The transmittance spectra showed two peaks for all the samples of the series. The first peak υ_1 (568-580 cm^{-1}) corresponds to the tetrahedral metal oxygen bond and second peak υ_2 (near 400 cm^{-1}) corresponds to octahedral metal oxygen bond in the ferrite structure [19].

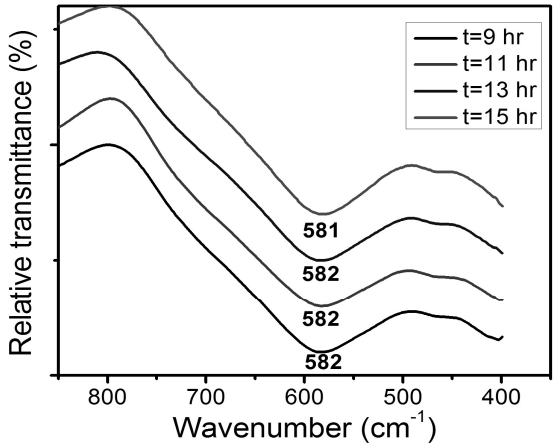

Fig.7. FTIR spectra of $Ni_{0.5}Cd_{0.5}Al_{0.1}Fe_{1.9}O_4$ ferrite series synthesized by ceramic method.

Conclusion

The $Ni_{0.5}Cd_{0.5}Al_{0.1}Fe_{1.9}O_4$ ferrite series with sintering time t=9, 11, 13, 15 hrs are successfully synthesized by ceramic method. The XRD studies confirm the single phase cubic spinel structure of the samples. The lattice parameter (8.47 Å - 8.48 Å) remains almost constant with increase in sintering temperature. Stacking fault coefficient observed to be very low, affirming the XRD peak position are at the expected value. The crystallite size is calculated using three different methods showed almost constancy (~50 nm) with increase in the sintering time. The SEM images show uniform size of the grains of size of the range of 1μm. The octahedral and tetrahedral structures are observed in morphology study. The grain size increased with increase in the sintering time. The EDAX studies confirm the presence of all the metal ions used in synthesis. The FTIR studies show two peaks υ_1(581-582 cm^{-1}) and υ_2(less than 400 cm^{-1}) confirming the presence of octahedral and tetrahedral positions inside the structure.

REFERENCES

1 Wrinkler, G., Crystallography, Chemistry and Technology of ferrites in Magnetic Properties of Materials, McGraw-Hill, London, UK, 1971.

2 Goldman, A. Modern Ferrite Technology, Springer, Boston Springer, Boston, 2006. doi: 0.1007/978-0-387-29413-1

3 Jauhar, S., Kaur, J., Goyal, A., Singhal, S., Tuning the properties of cobalt Ferrite: A road towards diverse applications. *RSC Adv*., 2016, Vol.6, no.100, pp. 97694-97719. doi 10.1039/C6RA21224G

4 Nedkov, I., Petkov, A., Cheparin, V., Microstructure and resonant properties of polycrystalline Sr-hexaferrite. J. Magn. Magn.Mater., 1990, Vol. 83, No.(1-3), pp. 430-432. doi10.1016/0304-8853(90)90573-9

5 Falk, R.B., Hooper,G.D., Elongated Iron-Cobalt: Ferrite, a New, Lightweight, Permanent Magnet Material. J. Appl. Phys. S, 1961, Vol. 32, No. 3, pp. 190-191. doi10.1063/1.2000396

6 Pon-On, W., Charoenphandhu, N., Tang, I.-M., Jongwattanapisan, P., Krishnamra, N., Hoonsawat, R., Encapsulation of magnetic $CoFe_2O_4$ in SiO_2 nanocomposites using hydroxyapatite as templates: A drug delivery system. Mater. Chem. Phys. 2011, Vol. 131, No. (1-2), pp. 485 – 494. doi 10.1016/j.matchemphys.2011.10.008

7 Bi, K., Zhu, W., Lei, M., Zhou, J., Magnetically tunable wideband microwave filter using ferrite-based metamaterials. *Appl. Phys. Lett*., 2015, Vol. 106, No. 17, pp. 173507(1-4). doi 10.1063/1.4918992

8 Hagfeldt, A., Graetzel, M., Light-Induced Redox Reactions in Nanocrystalline Systems. *Chemical Rev.*, 1995, Vol. 95, No. 1, pp. 49 – 68. doi 10.1021/cr00033a003

9 Farooq, H., Ahmad, M.R., Jamil, Y., Hafeez, A., Anwar, M. Structural, dielectric and magnetic properties of superparamagnetic zinc ferrite nanoparticles synthesized through coprecipitation technique, Kovove Mater., 2013, Vol. 51, pp. 305-310. doi 10.4149/km_2013_5_305

10 Kulkarni, A.B., Mathad, S.N., Synthesis and structural analysis of Co-Zn-Cd ferrite by Williamson-Hall and Size-Strain Plot Methods. Int. J. Self-Propag. High-Temp.Synth., 2018, Vol. 27, No. 1, pp. 37–43. doi10.3103/S106138621801003X

11 Kulkarni, A. B., Mathad, S. N., Variation in structural and mechanical properties of Cd-doped Co-Zn ferrites. Mater. Sci. Energy Techn., 2019, Vol. 2, No. 3, pp. 455 – 462. doi 10.1016/j.mset.2019.03.003

12 Lohar, K.S., Patange, S.M., Mane, M.L., Shirsath, S.E.,Cation distribution investigation and characterizations of $Ni_{1-x}Cd_xFe_2O_4$ nanoparticles synthesized by citrate gel process. J. Mol. Str., 2013, Vol. 1032, pp. 105-110. doi 10.1016/j.molstruc.2012.07.055

13 Raghavender, A.T., Jadhav, K.M., Dielectric properties of Al-substituted Co ferrite nanoparticles. *Bull. Mater. Sci.,* 2009, Vol. 32, No. 6, pp. 575 – 578. doi10.1007/s12034-009-0087-8

14 Pedrosa, F.J., Rial, J., Golasinski, K.M., Rodríguez-Osorio, M., Salas, G., Granados, D., Camarero, J., Bollero, A. Tunable nanocrystalline $CoFe_2O_4$ isotropic powders obtained by co-precipitation and ultrafast ball milling for permanent magnet applications. *RSC Adv.,* 2016, Vol. 6, No. 90, pp. 87282 – 87287. doi10.1039/C6RA15698C

15 Gomes, J.A., Sousa, M.H., Tourinho, F.A., Aquino, R., Silva, G.J., Depeyrot, J., Dubois, E., Perzynski, R. Synthesis of Core-Shell Ferrite Nanoparticles for Ferrofluids: Chemical and Magnetic Analysis. J. Phys. Chem. C, 2008, Vol. 112, No. 16, pp. 6220 – 6227. doi 10.1021/jp7097608

16 Zak, A.K., Abrishami, M.E., Majid, W.H.A., Yousefi ,R., Hosseini, S.M., X-ray analysis of ZnO nanoparticles by Williamson-Hall and size-strain plot methods. *Solid State Sci.*, 2011, Vol. 13, No. 1, pp.251 – 256. doi10.1016/j.solidstatesciences.2010.11.024

17 Tagliente, M.A., Massaro, M. Nucl. Instruments Methods. *Phys. Res. Sect. B Beam Interact. Mater. Atoms,* 2008, Vol. 266, No. 7, pp. 1055 – 1061. doi10.1016/j.nimb.2008.02.036

18 Prabhu, Y.T., Rao, K.V., Kumar V.S.S., Kumari B.S., X-Ray Analysis by Williamson-Hall and Size-Strain Plot Methods of ZnO Nanoparticles with Fuel Variation. World J. Nano Sci. Engg., 2014,V. 4, No.1, pp. 43743(1-8). doi 10.4236/wjnse.2014.41004

19 Pathan, A.T., Mathad, S.N., Shaikh, A.M., Infrared Spectral studies of Co^{2+} substituted Li-Ni-Zn Nano-structured Ferrites. Int. J. Self-Prop. High Temp. Synth., 2014, Vol. 23, No. 2, pp. 112-117. doi 10.3103/S1061386214020083

Article accepted for publication 27.07.2020